

**DTM PIXEL SCALE EFFECT ON PHOTOMETRY.** H. Sato<sup>1</sup>, B. W. Denevi<sup>2</sup>, M. S. Robinson<sup>1</sup>, and B. Hapke<sup>3</sup>,  
<sup>1</sup>Arizona State University, AZ 85287, USA (hsato@ser.asu.edu), <sup>2</sup>Johns Hopkins University Applied Physics  
 Laboratory, Laurel, MD 20723, USA, <sup>3</sup>University of Pittsburgh, Pittsburgh, PA 15260, USA.

**Introduction:** Thanks to observations from various instruments on multiple spacecraft, five lunar topography datasets are now available: Lunar Orbiter Laser Altimeter (LOLA) [1], Lunar Reconnaissance Orbiter Camera (LROC) Narrow Angle Camera (NAC) Digital Terrain Model (DTM) [2], LROC Wide Angle Camera (WAC) stereo DTM (GLD100) [3], SELENE (Kaguya) Laser Altimeter (LALT) [4], and Kaguya Terrain Camera (TC) DTM [5]. High-resolution DTMs enable calculation of accurate angles of incidence ( $i$ ) and emission ( $e$ ), which are the key factors in an accurate photometric normalization and the photometric analyses.

Sato et al. [6] demonstrated increased uncertainties in photometrically normalized reflectance mostly along the unresolved topographic undulations, based on the repeated WAC observations and the GLD100. Normalized reflectance derived from observations that span wide ranges of  $i$  and  $e$  can minimize such uncertainties [6], but this is not possible in areas such as at high latitudes where the range of  $i$  is limited (only high- $i$ ) and the pixel scale of the DTM may have a significant effect that has not yet been well studied. The sub-pixel scale topographic effect is modeled by employing the photometric roughness parameter  $\theta$  in the Hapke model [7]. However, how the unresolved topographies larger than the observation pixel scale (caused by low-resolution DTMs) can affect the photometric roughness is not well understood. Laboratory experiments showed no strong link between the topography and  $\theta$  [8,9], but this has not yet been tested using actual planetary remote sensing datasets.

In this study, we derive  $\theta$  and normalized radiance factor ( $nI/F$ ) [7] from WAC images using DTMs with various pixel scales, to clarify 1) how the normalized images are affected and 2) if/how the calculation of  $\theta$  is controlled by the DTM resolution.

**Methodology:** We used ~84 sets of near-global WAC 7-band (321-689 nm) data. Each observation was acquired with different lighting and viewing conditions owing to the WAC's wide field-of-view and the evolution of LRO's orbit, resulting in a rich spectral-photometric dataset. The observations were radiometrically calibrated [10] to 32-bit  $I/F$ . As the DTM datasets, we used a NAC DTM (5 m/pixel), a TC DTM (originally ~8 m/pixel, down-sampled to 100 m/pixel), and the GLD100 (100 m/pixel). To purely examine the pixel-scale effect, we down-sampled the

NAC DTM to various scales down to 2000 m/pixel. The elevations at nine surrounding points along each pixel were used to calculate the slope. To avoid the sharp offset along the pixel boundaries of low-resolution DTMs, linear interpolation was applied when reading DTMs with pixel scales >150 m.

We selected two test sites, one in the middle of the highlands (41° to 44°N, 167° to 169°E) where possible impact melts were extensively distributed [11]. Another is at the north portion of Oceanus Procellarum (42° to 45°N, 309° to 311°E) near Rima Sharp. In both sites, relatively large NAC DTM mosaics are available.

For each 1° latitude by 1° longitude tile, we calculated the  $w$  (single scattering albedo),  $b$  (Henyey-Greenstein 2-lobed phase function parameter),  $hs$  (angular width of Shadow Hiding Opposition Effect), and  $\theta$  (roughness parameter) with the parameter calculation procedure developed by [6] using various DTMs. For each DTM, we re-calculated the  $i$  and  $e$  angles and derived the Hapke parameters. Only the visible band observations from the 50 km fixed-orbit period (relatively higher spatial resolutions; original pixel scale <110 meters) were used to test the resolution effect of the DTMs. We normalized each WAC image using the  $i$  and  $e$  and the Hapke

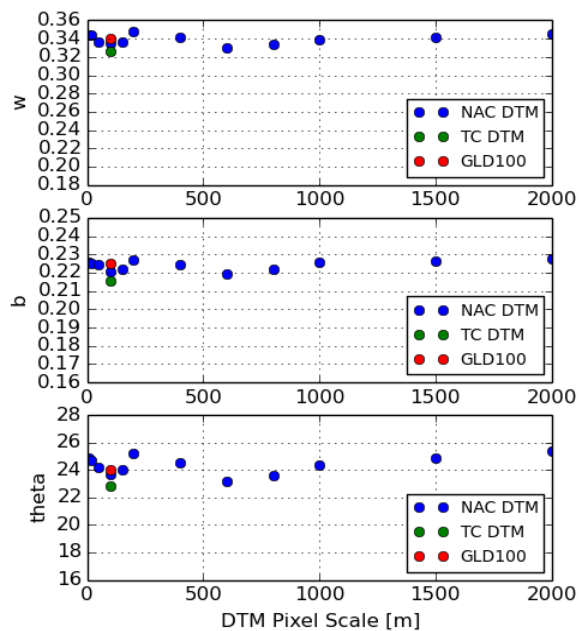


Figure 1. Derived Hapke parameters for a highland tile (1° by 1°) centered at 43.5°N, 167.5°E; 689 nm band. Y-axes are stretched to the derived parameter ranges inside the highland sampling sites.

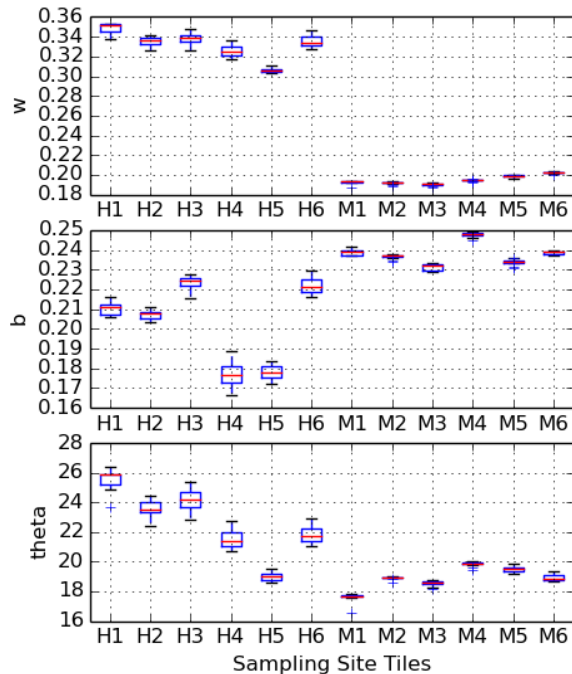


Figure 2. Boxplot of the derived Hapke parameters for each tile (based on various DTMs) in the highland (H1-6) and the mare (M1-6) sampling sites.

parameters derived from each DTM. Then we examined the relative changes of the  $nI/F$  and  $\theta$  as a function of the DTM pixel scales.

**Results and Discussions:** The derived Hapke parameters including the roughness parameter  $\theta$ , based on various DTM pixel scales (Fig. 1), have minor variations but no remarkable trend with the DTM pixel scale. This indicates that the uncertainties of local  $i$  and  $e$  angles caused by unresolved topographic variations do not dominantly affect the  $\theta$  values. This result is consistent with laboratory experiments [8,9]. We also derived the Hapke parameters from data where  $i$  and  $e$  were calculated based on an ellipsoid surface. With no DTM, extreme values of photometric parameters were often found. Thus even a low-resolution DTM, up to 10 times the image pixel scale, is preferable to simply using an ellipsoid.

Compared to the minor variations of Hapke parameters caused by the DTM pixel scales, the differences between the tiles or between the highland and the mare are more significant (Fig. 2). Thus the actual surface material properties, rather than the super-pixel scale roughness or an accuracy of the DTM, is dominantly controlling the Hapke parameters.

The  $nI/F$ s are significantly altered by the DTM pixel scale (Fig. 3). Using the  $nI/F$  based on the original NAC DTM (5 m/pixel) as a standard, we divided all the  $nI/F$  based on various DTMs. As the

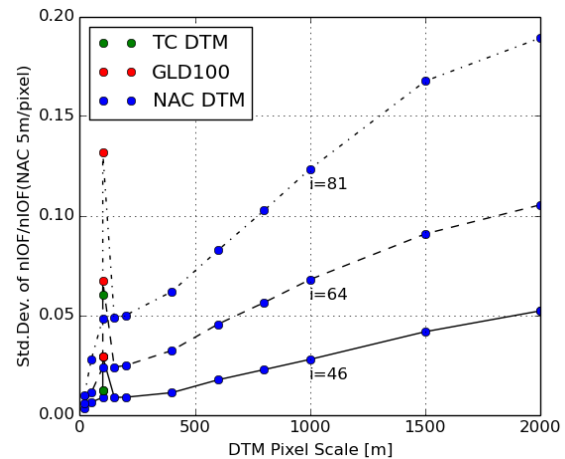


Figure 3. Standard deviation of the ratios of  $nI/F$  based on various DTMs over  $nI/F$  based on the NAC DTM (5 m/pixel) in 689 nm band and in the same highland tile as Fig. 1. Each line corresponds to one WAC image with different incidence angles (averaged value).

DTM pixel scale increases, the areas with unresolved topography increase, resulting in locally low/high  $nI/F$ s relative to the standard  $nI/F$  (thus increased standard deviation in Fig. 3). This effect increases with  $i$  angles. The GLD100 and TC DTM show larger standard deviation than the NAC DTM down-sampled to the similar scales, because the effective pixel scales of both DTMs are much lower and probably have different roughness compared to the emulated one by down-sampling the higher spatial resolution DTM.

The ratio values of 415/689 nm bands based on various DTMs showed a similar trend as Fig. 3 (although the amplitude is small, up to  $\sim 0.1$  in  $i=81$  curve), indicating that the colors can be controlled by the DTM's pixel scale. This DTM dependent color artifact effect will be increased toward the pole since the high latitudes receive only high- $i$  angles. Thus the studies such as the latitudinal trends in the colors will require extra caution.

#### References:

- [1] Smith D. E. et al. (2009) *Space Sci. Rev.* 150, 209-241.
- [2] Henriksen M. et al (2017) *Icarus*, v283, p122-137.
- [3] Scholten F. et al. (2012) *JGR*, 117, E00H17.
- [4] Araki, H. et al. (2009) *Science* 323, 897.
- [5] Haruyama, J. et al. (2014) *LPSC abst.* #1304.
- [6] Sato H. et al. (2014) *JGR*, 119(8), 1775-1805.
- [7] Hapke B. (2012) *Theory of Reflectance and Emittance Spectroscopy*, Cambridge Univ. Press.
- [8] Cord et al. (2003) *Icarus*, 165(2), 414-427.
- [9] Shepard and Helfenstein (2007) *JGR*, 112, E03001.
- [10] Mahanti P. et al. (2015) *Space Sci. Rev.*, DOI 10.1007/s11214-015-0197-0.
- [11] Robinson M.S. et al. (2016) *Icarus*, v273, 15, p121-134.